Kolmogorov's refined similarity hypotheses for turbulence and general stochastic processes

G. Stolovitzky and K. R. Sreenivasan

Mason Laboratory, Yale University, New Haven, Connecticut 06520-8286

Kolmogorov's refined similarity hypotheses are shown to hold true for a variety of stochastic processes besides high-Reynolds-number turbulent flows, for which they were originally proposed. In particular, just as hypothesized for turbulence, there exists a variable V whose probability density function attains a universal form. Analytical expressions for the probability density function of V are obtained for Brownian motion as well as for the general case of fractional Brownian motion—the latter under some mild assumptions justified *a posteriori*. The properties of V for the case of antipersistent fractional Brownian motion with the Hurst exponent of $\frac{1}{3}$ are similar in many details to those of high-Reynolds-number turbulence in atmospheric boundary layers a few meters above the ground. The one conspicuous difference between turbulence and the antipersistent fractional Brownian motion is that the latter does not possess the required skewness. Broad implications of these results are discussed.

CONTENTS

I. INTRODUCTION

A. Kolmogorov's hypotheses of 1941

A cornerstone of our understanding of high-Reynolds-number fluid turbulence is the phenomenological theory put forward by Kolmogorov (1941a). Kolmogorov visualized that energy gets injected into a fluid flow at some large scale L, either by mechanical or thermomechanical means, or by means of a large-scale instability. He further visualized that the fluid motion at scale L would become unstable and lose its energy to neighboring smaller scales without directly dissipating it into heat. At high Reynolds numbers, this process is supposed to repeat itself until one reaches a sufficiently small scale (now known as the Kolmogorov scale) at which no further instabilities are possible, and the energy is directly dispersed to heat by viscous action. Kolmogorov assumed that the rate of energy input at the large scales and of energy dissipation at the small scales are equal to each other and to the energy transfer rate across the spectrum of intermediate scales. The anisotropy and inhomogeneity at the large scales are thought to diminish with decreasing scale, so that scales far smaller than L become statistically isotropic and homogeneous, this being the hypothesis of local isotropy. Kolmogorov further assumed that the energy dissipation rate remains finite in the limit of infinite Reynolds number.

Kolmogorov formulated this physical picture in terms of the following two well-known hypotheses:

(1) The scales of motion $r \ll L$ that dissipate most of the turbulent energy are locally isotropic, and their statistics are determined uniquely by $\langle \varepsilon \rangle$, the global average of the energy dissipation rate per unit mass, ε, and by the kinematic viscosity coefficient ν.

One can construct, from $\langle \varepsilon \rangle$ and ν, a length scale $\eta = (\nu^3/\langle \varepsilon \rangle)^{1/4}$ and a velocity scale $(\nu\langle \varepsilon \rangle)^{1/4}$, which are the Kolmogorov length and velocity scales, respectively.[1] The first hypothesis is equivalent to the assertion that the dissipative scales are characterized completely by η and v and are independent of the large-scale details of turbulence. For any positive integer n, dimensional analysis then yields the result that

$$\langle [\Delta u]^n \rangle = v^n f_n(r/\eta) , \tag{1}$$

where $\Delta u(r) = u(x+r) - u(x)$, u being the x component of the velocity vector $\mathbf{u}(\mathbf{x})$ with separation distance r measured along x, and where the functions $f_n(r/\eta)$ are independent of the Reynolds number and of the details of energy injection.

(2) For the so-called inertial range scales $\eta \ll r \ll L$ (assuming that such a range exists), the viscosity becomes irrelevant and the statistics of $\Delta u(r)$ depend only on the global average of the energy dissipation rate, $\langle \varepsilon \rangle$.

The second hypothesis means that the functions f_n in Eq. (1) have to assume a form that will suppress ν (which manifests indirectly through v and η). Elementary ma-

[1]Note that the dimensions of ε are (velocity)^2/time or (velocity)^3/length. The Reynolds number $v\eta/\nu$, based on the Kolmogorov scales, is unity by construction—this being the reason why turbulence subsides at scales much smaller than η.

 0034-6861/94/66(1)/229(12)/$06.20

nipulations of Eq. (1) yield the result that

$$\langle [\Delta u]^n \rangle = K_n (\langle \varepsilon \rangle r)^{n/3} , \tag{2}$$

where the coefficients K_n are some suitable constants. With the expectation that the K_n are universal (in the sense that they are independent of all large-scale features), Eq. (2) expresses the global universality of turbulence in the inertial range. The statements (1) and (2) have equivalent forms in their spectral representation. The encyclopedic work by Monin and Yaglom (1971) can be consulted for further details.

B. Intermittency corrections

The arguments used to derive Eqs. (1) and (2) ignore many facets of turbulence, in particular, the intermittency of ε—by which one means that ε shows extreme variability in its spatial distribution. In the limit of infinitely large Reynolds number, ε is thought to be ill defined over most of the space. In particular, intermittency of ε renders the use of the global average $\langle \varepsilon \rangle$ insufficiently representative of its behavior. The first recognition of the importance of intermittency is traced to a comment by Landau (see, for instance, Landau and Lifshitz, 1963). Although Landau's comment literally referred to the nonuniversality that may arise from averaging ε over many nonuniversal large scales, Kolmogorov (1962) attributed the recognition of intermittency effects to Landau.

Experiments (e.g., Anselmet *et al.*, 1984; Stolovitzky *et al.*, 1993) have shown Eq. (2) not to be correct in general. One has, instead,

$$\langle [\Delta u]^n \rangle = K_n (\langle \varepsilon \rangle L)^{n/3} (r/L)^{\zeta_n} , \tag{3}$$

where $\zeta_n = n/3 - \mu_n$, and the so-called intermittency exponents μ_n are treated as corrections to the classical scaling exponents $n/3$ [see Eq. (2)]. The only precise result (Kolmogorov, 1941b) known from dynamical equations is that $\mu_3 = 0$. Experiments show that $\mu_2 < 0$ and $\mu_n > 0$ for all $n > 3$, and that the μ_n become increasingly important as n increases. Much effort has been expended in modeling this behavior. For a survey of these effects, see Meneveau and Sreenivasan (1991).

C. The refined similarity hypotheses

Kolmogorov's (1962) refinement of his earlier hypotheses was based on a proposal by Obukhov (1962), who recognized that the role of the global average in the earlier hypotheses should be assigned to local averages of the energy dissipation rate. The proposal was, effectively, to divide the spatial domain into a collection of ensembles, each of them characterized by a fixed value of the locally averaged energy dissipation rate ε_r, where ε_r is the average of ε over a volume of linear dimension r. The refined hypotheses are stated below. (An entirely new third hypothesis was added, but we shall not consider it here.)

1. The first refined hypothesis

Over a range of scales r such that $r \ll L$, the probability density function of the stochastic variable

$$V = \frac{\Delta u(r)}{(r\varepsilon_r)^{1/3}} \tag{4}$$

depends only on the local Reynolds number $\mathrm{Re}_r = r(r\varepsilon_r)^{1/3}/\nu$.

2. The second refined hypothesis

If $\mathrm{Re}_r \gg 1$, the probability density function of V does not depend on Re_r either, and is therefore universal. (Note: The hypothesis does not specify the probability density function itself.)

The refined hypotheses have served as a vital reference point in the research of high-Reynolds-number turbulence. Although it was shown recently (Stolovitzky *et al.*, 1992) that the probability density function of V also depends on r when r is small, several aspects of the hypotheses have been verified experimentally (Praskovsky, 1992; Stolovitzky *et al.*, 1992; Thoroddsen and Van Atta, 1992) as well as by direct numerical simulations of turbulence (Chen *et al.*, 1993; Hosokawa, 1993). This is a remarkable situation because $\Delta u(r)$ is a purely inertial range quantity when r is an inertial range separation distance, whereas ε_r is a mixed quantity (the dissipation rate averaged over an inertial range scale). In view of the large scale separation believed to exist at high Reynolds numbers, it is indeed surprising (Kraichnan, 1974) that their ratio (4) is essentially universal. (We may note explicitly that universality here means that the probability density function of V is independent of r and ε_r.) Further, in spite of their widespread use and significant experimental support, the refined hypotheses have not been derived from first principles. Because of this, it is particularly difficult to see how much of their content is specific to fluid turbulence, or rather a property of general stochastic processes. It is not clear whether any broad statistical principle transcending the details of turbulent motion requires the applicability of the refined hypotheses. This paper takes a step towards clarifying the situation.

D. The scope of the paper

The intent of this paper is to show that a large part of the refined hypotheses can be derived from general stochastic principles unrelated to the Navier-Stokes equations. We cast the refined hypotheses in terms of general stochastic processes and show that they hold for the classical Brownian motion as well as for the antipersistent fractional Brownian motion (Mandelbrot and Van Ness, 1968); that is, we demonstrate for these cases the existence of a universal stochastic variable, just as Kolmogorov hypothesized for turbulence. Recall that Browni-

an motion results from summing uncorrelated random increments and that the fractional Brownian motion extension of the classical Brownian process consists of correlated increments. If we imagine the process occurring in a one-dimensional spatial domain, with $Z(x)$ denoting the value of a realization of the fractional Brownian motion at the spatial location x, we say that $Z(x)$ is a fractional Brownian motion with a Hurst exponent H ($0 \le H \le 1$) if the distribution of the increments $\Delta Z(r)=Z(x+r)-Z(x)$ is Gaussian with zero mean and with the variance $\langle \Delta Z(r)^2 \rangle \sim r^{2H}$ for large r. (To avoid confusion, we use $Z(x)$ for the fractional Brownian motion and $u(x)$ for the turbulent velocity.) A fractional Brownian motion with $0<H<1/2$ is said to be antipersistent in the sense that positive increments for some x imply (statistically) negative increments for $x+r$, and vice versa. The range $1/2<H<1$ is called the persistent range: Positive increments for some x imply (statistically) positive increments for $x+r$. The special value $H=1/2$ yields the familiar Brownian motion, for which successive increments are independent [see details, for example, in Voss (1985, 1988)]. We shall derive an exact closed-form expression for the probability density function of an equivalent of V for the classical Brownian motion, as well as for the fractional Brownian motion—the latter under some mild assumptions that are justified *a posteriori*. We shall show that the fractional Brownian motion result for a Hurst exponent $H=1/3$ agrees in large measure with the experimental probability density function of V for turbulence. A conspicuous difference between turbulence and other stochastic processes will be pointed out, together with some implications of the results.

II. A CONVENIENT RESTATEMENT OF THE REFINED HYPOTHESES

The energy dissipation rate per unit mass in three-dimensional turbulence is exactly written as

$$\varepsilon=(\nu/2)\sum_{i,j}[(\partial u_i/\partial x_j)^2+(\partial u_j/\partial x_i)^2] , \tag{5}$$

where the x_i ($i=1-3$) are the Cartesian components of the vector position $\mathbf{x}$ and the u_i are the components of the velocity $\mathbf{u}$ in the same coordinate system. Local isotropy allows the global *average* of the full energy dissipation to be expressed in terms of the one-dimensional velocity derivative as $\langle \varepsilon \rangle = 15\nu\langle (du/dx)^2 \rangle$ (Taylor, 1935). It is traditional in the turbulence literature to assume on this basis that ε and $(du/dx)^2$ have the same scaling behavior. This assumption is not strictly true because the statement about equality of averages cannot generally be translated to one about equality of scaling properties. However, Chen *et al.* (1993) have shown that a consideration of the full expression for ε does not significantly alter the conclusions about the refined hypotheses,[2] which can therefore be stated as a relation between the velocity increments

$$\Delta u(r)=\int_x^{x+r}\frac{du}{dx}\,dx \tag{6}$$

and the energy dissipation rate in a segment of linear size r, given by

$$r\varepsilon_r=15\nu\int_x^{x+r}\left[\frac{du}{dx}\right]^2 dx . \tag{7}$$

Given that $\Delta u(r)$ and $r\varepsilon_r$ are both functionals of the velocity gradient [see Eqs. (6) and (7)], they are correlated variables in general.

Discretizing the integrals (6) and (7) and normalizing all lengths by the Kolmogorov scale η and all velocities by the Kolmogorov velocity v, we may write Eqs. (6) and (7), respectively, as

$$\frac{\Delta u(r)}{K(\eta\langle\varepsilon\rangle)^{1/3}}\approx\sum_{i=1}^{p}X_i=S_p \tag{8a}$$

and

$$\frac{r\varepsilon_r}{15K\eta\langle\varepsilon\rangle}\approx\sum_{i=1}^{p}X_i^2=Y_p^2 . \tag{8b}$$

Here, $X_i=du/dx|_{x_i}\eta/(\eta\langle\varepsilon\rangle)^{1/3}$ and $p=r/K\eta$. The variables X_i are simply the normalized (and smooth) velocity increments across a distance $K\eta$, with K being the number of Kolmogorov scales over which smoothness obtains. Because of the intermittency of ε, the size of the smooth regions varies from place to place—being small when ε_r is large and vice versa. In the sums (8a) and (8b), X_i is evaluated at location x_i and the following X_{i+1} at $x_{i+1}=x_i+K\eta$.

In the example of the fractional Brownian motion $Z(x)$, X_i represents the increments $\Delta Z=Z(x_i+1)-Z(x_i)$ and p the ratio r/K (without reference to the scale η). The definitions apply here as in Eqs. (8), yielding

$$\Delta Z(r)/K\approx S_p \tag{9a}$$

and

$$w_r/15K\approx Y_p^2 , \tag{9b}$$

---

[2]Chen *et al.* (1993) obtained the full dissipation from a direct numerical solution of the Navier-Stokes equations, and demonstrated that the one-dimensional representation of the full dissipation given by Eq. (5) is adequate in the context of the refined hypotheses. However, the simulations of Chen *et al.* (like other numerical solutions of Navier-Stokes equations) pertain to low Reynolds numbers. If the demonstration of these authors were to hold for high Reynolds number as well, the experimental work—which, by necessity, is almost always restricted to measuring only the one-dimensional surrogate of Eq. (5)—would be on firmer ground. This would be true of the present work as well.

with $w_r=15\sum_1^r[Z(x+i)-Z(x+i-1)]^2$. The new dissipationlike parameter w_r is defined to coincide with $r\varepsilon_r$ in the case of turbulence [see Eq. (7)]. In analogy to the stochastic variable V of Eq. (4), we wish to study the variable

$$V_{\rm fBm}=\frac{\Delta Z(r)}{w_r^H}=\frac{K^{1-H}}{15^H}\frac{S_p}{Y_p^{2H}}\ , \tag{10}$$

in particular, its conditional probability density function for given values of w_r and r. (For later notational simplicity, this conditional probability density function will be designated as the pdf conditioned on w_r and r.) In particular, we wish to prove that the pdf of $V_{\rm fBm}$ conditioned on w_r tends to a universal form for large w_r and r. This is the appropriate statement of the problem in the context of the refined hypotheses.

In the following sections, we develop a formalism for computing the conditional pdf of $V_{\rm fBm}$ for the general case. We first provide results for an independent Gaussian X_i as well as for a non-Gaussian independent X_i, and subsequently for fractional Brownian motion. We shall then return to the problem of turbulence to examine the implications of the results just mentioned. To help sustain focus, it may be useful to reiterate here the central aspect of the approach, as well as to anticipate its principal conclusion. The approach is to demonstrate that most aspects of the refined similarity hypotheses, particularly the existence of the universal stochastic variable V of Eq. (4), hold for Gaussian processes (with either uncorrelated or correlated increments) as well as for non-Gaussian uncorrelated processes. The only significant point of departure from turbulence concerns the (relatively small but important) skewness of the pdf of the variable V.

III. THE GENERAL PROCEDURE

We start by studying the joint pdf of S_p and Y_p at fixed p, represented by $P_2(S_p,Y_p;p)$. If the X_i are taken to be components of the p-dimensional vector $\mathbf{X}=(X_1,\ldots,X_p)$, then $\mathbf{X}$ belongs to both the hyperplane $\sum_{i=1}^p X_i=S_p$ and the hypersphere $\sum_{i=1}^p X_i^2=Y_p^2$. It will prove convenient to rotate the coordinate system X_j to a new system U_j so that one of the new axes (say, U_1) is orthogonal to the hyperplane. The change of coordinates is governed by

$$U_j=\sum_{i=1}^p R_{ij}X_i\ , \tag{11}$$

where R_{ij} is an orthogonal matrix with $R_{1j}=1/\sqrt{p}$. (The remaining components R_{kj}, $2\le k\le p$, can be computed using, for example, a Gram-Schmidt orthogonalization procedure, but are irrelevant for our immediate purposes.) The second equality conditions in Eqs. (8) can now be rewritten as

$$U_1=\frac{S_p}{\sqrt{p}} \tag{12a}$$

and

$$\sum_{i=1}^p U_i^2=Y_p^2\ . \tag{12b}$$

Now, in terms of the U variables, we may write the joint pdf as

$$\begin{aligned}P_2(S_p,Y_p;p)=&\int_{R^p}dU_1\ldots dU_p P_U(U_1,\ldots,U_p)\\ &\times\delta(S_p-\sqrt{p}\,U_1)\\ &\times\delta\left[Y_p-\left[\sum_{i=1}^p U_i^2\right]^{1/2}\right]\ ,\end{aligned} \tag{13}$$

where $\delta(x)$ is Dirac's delta function, $P_U(U_1,\ldots,U_p)$ is the joint pdf of $U_1,\ldots,U_p$ given by

$$\begin{aligned}&P_U(U_1,\ldots,U_p)\\ &\quad=P_X[X_1(U_1,\ldots,U_p),\ldots,X_p(U_1,\ldots,U_p)]\ ,\end{aligned} \tag{14}$$

and $P_X(X_1,\ldots,X_p)$ is the joint pdf of $X_1,\ldots,X_p$. In writing Eq. (14) we have used the fact that the Jacobian of the transformation given by Eq. (11) is unity.

At this point, we introduce a p-dimensional spherical polar coordinate system related to the Cartesian systems $(U_1,U_2,\ldots,U_p)$ through (see, for example, Sommerfeld, 1949, Appendix IV, p. 227)

$$\begin{aligned}U_1(\rho,\theta,\phi_1,\ldots,\phi_{p-2})&=\rho\cos\theta\ ,\\ U_2(\rho,\theta,\phi_1,\ldots,\phi_{p-2})&=\rho\sin\theta\cos\phi_1\ ,\\ U_3(\rho,\theta,\phi_1,\ldots,\phi_{p-2})&=\rho\sin\theta\sin\phi_1\ ,\\ U_4(\rho,\theta,\phi_1,\ldots,\phi_{p-2})&=\rho\sin\theta\sin\phi_1\cos\phi_2\ ,\\ &\cdots\ ,\\ U_{p-1}(\rho,\theta,\phi_1,\ldots,\phi_{p-2})&=\rho\sin\theta\sin\phi_1\cdots\sin\phi_{p-3}\cos\phi_{p-2}\ ,\\ U_p(\rho,\theta,\phi_1,\ldots,\phi_{p-2})&=\rho\sin\theta\sin\phi_1\cdots\sin\phi_{p-3}\sin\phi_{p-2}\ ,\end{aligned} \tag{15}$$

where $0<\rho<\infty$, $0<\theta<\pi$, $0<\phi_i<\pi$ for $i=1,\ldots,p-3$ and $-\pi<\phi_{p-2}<\pi$. The Jacobian of this transformation is

$$\begin{aligned}&\frac{\partial(U_1,\ldots,U_p)}{\partial(\rho,\theta,\phi_1,\ldots,\phi_{p-2})}\\ &\quad=\rho^{p-1}(\sin\theta)^{p-2}(\sin\phi_1)^{p-3}\cdots(\sin\phi_{p-3})\ .\end{aligned} \tag{16}$$

The integral (13) can be partially performed in polar coordinates; noting that $(\sum_{i=1}^p U_i^2)^{1/2}=\rho$ and $U_1=\rho\cos\theta$, we first integrate over ρ and then over θ, to obtain

$$P_2(S_p,Y_p;p)=\frac{Y_p^{p-2}}{\sqrt{p}}\left[1-\frac{S_p^2}{pY_p^2}\right]^{(p-3)/2}\Xi(Y_p,S_p;p)\ , \tag{17}$$

where

$$\Xi(Y_p,S_p;p)=\int_{\Omega_\phi} d\omega_\phi P_U\left[\frac{S_p}{\sqrt{p}},U_2(Y_p,\theta^*,\theta's),\ldots,U_p(Y_p,\theta^*,\phi's)\right],$$
$$\theta^*=\cos^{-1}\left[\frac{S_p}{\sqrt{p}\,Y_p}\right], \tag{18}$$

and

$$d\omega_\phi=d\phi_1\cdots d\phi_{p-3}d\phi_{p-2}(\sin\phi_1)^{p-3}\cdots(\sin\phi_{p-3}) .$$

All the results so far are exact. The main task that remains now is the evaluation of the integral (18) and thus the joint pdf P_2 of S_p and Y_p. From this joint pdf, one may compute the pdf of S_p conditioned on Y_p as

$$P_1(S_p|Y_p;p)=\frac{P_2(S_p,Y_p;p)}{\int dS_p P_2(S_p,Y_p;p)} \tag{19}$$

and compare its properties with those expected from the refined hypotheses. This is our central purpose. Various special cases of Eq. (19) will now be considered.

IV. NORMALLY DISTRIBUTED INDEPENDENT X_i: THE CLASSICAL BROWNIAN MOTION

Let the X_i be identically distributed independent random variables with Gaussian density with zero mean and variance σ^2. We then have the following exact result. (Even though $H=1/2$ for this example, it is instructive to leave it as a variable for comparison with the general case of Sec. VI.)

Theorem: For any integer $p\geq 2$, the probability density function of $V_{Bm}=S_p/Y_p^{2H}$ conditioned on Y_p is independent of Y_p only when $H=1/2$. For this case, the conditional pdf assumes the form

$$f(V_{Bm}|Y_p;p)=\frac{1}{\sqrt{p}\,\Omega_\theta(p)}\left[1-\frac{V_{Bm}^2}{p}\right]^{(p-3)/2},$$
$$V_{Bm}^2<p , \tag{20}$$

where $\Omega_\theta(p)=(\pi/2p)[\Gamma(p-1)]/[\Gamma(p/2)]^2$, written in terms of the gamma function $\Gamma(x)$.

Proof: For this special case, we can perform the integral (18) completely. The assumption of Gaussianity and independence implies that the joint pdf $P_X(X_1,\ldots,X_p)=\exp(-\sum_1^p X_i^2/2\sigma^2)/(2\pi\sigma^2)^{p/2}$. Equation (14) then leads to the result $P_U(U_1,\ldots,U_p)=\exp(-\sum_1^p U_i^2/2\sigma^2)/(2\pi\sigma^2)^{p/2}$, whereby the integrand in Eq. (18) becomes independent of the integration variables ϕ, amounting to $\exp(-Y_p^2/2\sigma^2)/(2\pi\sigma^2)^{p/2}$. We thus find that

$$P_2(S_p,Y_p;p)=\Omega_\phi(p)\left[1-\frac{S_p^2}{pY_p^2}\right]^{(p-3)/2}\times\frac{\exp(-Y_p^2/2\sigma^2)}{(2\pi\sigma^2)^{p/2}} , \tag{21}$$

where $\Omega_\phi(p)=\pi(p-1)/\Gamma[(p-1)/2]$ is the integral over ϕ_1 through ϕ_{p-2} of $(\sin\phi_1)^{p-3}\cdots(\sin\phi_{p-3})$. The probability of S_p conditioned on Y_p is then computed according to Eq. (19) to be

$$P(S_p|Y_p;p)=\frac{1}{\sqrt{p}\,Y_p\Omega_\theta(p)}\left[1-\frac{S_p^2}{pY_p^2}\right]^{(p-3)/2} , \tag{22}$$

where $\Omega_\theta(p)=\int_0^\pi(\sin\theta)^{p-2}d\theta$, as expressed in closed form in the statement of the theorem. From change of variables to $V_{Bm}=S_p/Y_p^{2H}$, one obtains the pdf of V_{Bm} conditioned on Y_p to be

$$f_H(V_{Bm}|Y_p;p)=\frac{1}{\sqrt{p}\,Y_p^{1-2H}\Omega_\theta(p)}\times\left[1-\frac{V_{Bm}^2}{pY_p^{2-4H}}\right]^{(p-3)/2} . \tag{23}$$

It is easily seen that $f_H(V_{Bm}|Y_p;p)$ is independent of Y_p only for $H=1/2$, in which case $f_{1/2}(V_{Bm}|Y_p;p)$ has the form stated in the theorem. The theorem can be restated, for the case of independent velocity increments, in terms analogous to Kolmogorov's hypotheses:

(H1) The pdf of the stochastic variable $V_{Bm}=S_p/Y_p$ conditioned on Y_p depends only on p.

(H2) When $p\gg 1$, the pdf of V_{Bm} becomes independent of p; in fact, it tends to the normal distribution.

Plots of $f(V_{Bm}|Y_p;p)$ for different values of p are shown in Fig. 1. These functions are nonzero only over the interval $(-\sqrt{p},\sqrt{p})$. The distribution for $p=2$ is clearly bimodal; that for $p=3$ is uniform between $-\sqrt{3}$ and $\sqrt{3}$. The trend towards a Gaussian distribution sets in for larger p; there is negligible departure from Gaussian (dashed line) for $p=50$.

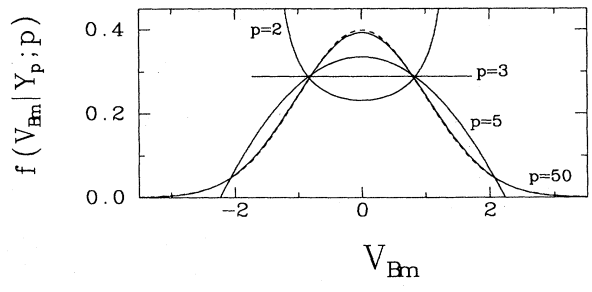

FIG. 1. Plots of $f(V_{Bm}|Y_p;p)$ for different values of the parameter p when the random increments X_i are assumed to be independent and Gaussian.

V. NON-GAUSSIAN INDEPENDENT PROCESSES

We now explore the consequences of relaxing the hypotheses that the X_i are normally distributed, assuming still that they are independent.

Let $V_{nG}=S_p/Y_p$ and the X_i be independent random variables with zero odd-order moments and nondivergent even-order moments. These conditions imply that $\langle V_{nG}^n | Y_p;p \rangle = 0$ for odd n. We wish to show that, for $p \gg 1$ and even $n \geq 2$,

$$\langle V_{nG}^n | Y_p;p \rangle \approx (n-1)!! , \tag{24}$$

where $(n-1)!!=(n-1)(n-3)\cdots 3.1$. Equation (24) implies that V_{nG} is a Gaussian random variable with zero mean and unity variance. In particular, for $p \gg 1$, the pdf of V_{nG} is independent of p and Y_p. For an informal proof of the result, write the nth power of S_p as

$$S_p^n = \sum_{i_1+\cdots+i_p=n} \frac{n!}{i_1!\cdots i_p!} X_1^{i_1}\cdots X_p^{i_p} , \tag{25}$$

where the sum extends over all the possible values $0 \leq i_j \leq n$ with $\sum_1^p i_j = n$, and we note that, when $p \gg 1$, most of the contribution to S_p^n is likely to come from terms containing even i_j (because the terms with odd i_j generally possess alternating signs and are likely to cancel out). It is clear that the terms with $i_j=0$ or 2 dominate the sum, so that we may rewrite Eq. (25) as

$$S_p^n \approx \sum_{i_1+\cdots+i_p=n} \frac{n!}{2^{n/2}} X_1^{i_1}\cdots X_p^{i_p} , \tag{26}$$

where i_j takes only the values 0 or 2. This statement could be made more rigorous by bounding the errors made in this approximation, but this will not be attempted here.

A similar analysis for Y_p, with i_j assuming only values of 0 or 1 in Eq. (27a) and values of 0 or 2 in Eq. (27b), would yield

$$Y_p^n \approx \sum_{i_1+\cdots+i_p=n/2} (n/2)! X_1^{2i_1}\cdots X_p^{2i_p} \tag{27a}$$

$$\approx \sum_{i_1+\cdots+i_p=n} (n/2)! X_1^{i_1}\cdots X_p^{i_p} . \tag{27b}$$

Comparing Eqs. (26) and (27b), we obtain

$$\langle S_p^n | Y_p;p \rangle \approx \frac{n!}{2^{n/2}(n/2)!} Y_p^n . \tag{28}$$

Noting that $n!/[2^{n/2}(n/2)!]=(n-1)!!$, we restate Eq. (28) as

$$\langle V_{nG}^n | Y_p;p \rangle \approx (n-1)!! \tag{29}$$

for $p \gg 1$, as required. We thus conclude that in this limit the pdf of V_{nG} conditioned on Y_p is independent of p and Y_p. Actually, it tends to be Gaussian with zero mean and unit variance.

We now illustrate these results numerically. For definiteness, we consider that the variables X_i are distributed according to an exponential density g, i.e.,

$$g(X)=\tfrac{1}{2}\exp(-|X|) , \tag{30}$$

for which $\langle X^2 \rangle = 2$ and $\langle Y_p \rangle = 2p$. We have computed the pdfs $h(V_{nG}|Y_p;p)$ of $V_{nG}=S_p/Y_p$ conditioned on Y_p for different values of p. The values of the conditioning parameter Y_p are taken as windows of size $\langle Y_p \rangle /3$ centered at the values indicated in Fig. 2. Figure 2(a) shows bimodal distributions for $p=3$ with some dependence on Y_p. Recalling that the equivalent distribution for Gaussian X_i is uniform for $p=3$, we conclude that the conditional distributions of V_{nG} for small p do depend on the distribution of X_i. For $p=10$ [Fig. 2(b)], the distributions already exhibit Gaussian-like behavior, while for $p=50$ [Figs. 2(c) and 2(d)] they hardly differ from Gaussian. As p increases, the differences among the various curves corresponding to different values of Y_p diminish. In particular, for $p=50$, all four curves coalesce quite well.

Again, the behavior just discussed can be described in terms analogous to Kolmogorov's similarity hypotheses: (H1) the pdf of V_{nG} conditioned on Y_p depends on Y_p and p; (H2) for $p \gg 1$, it tends to a Gaussian with zero mean and unit variance. This behavior is independent of

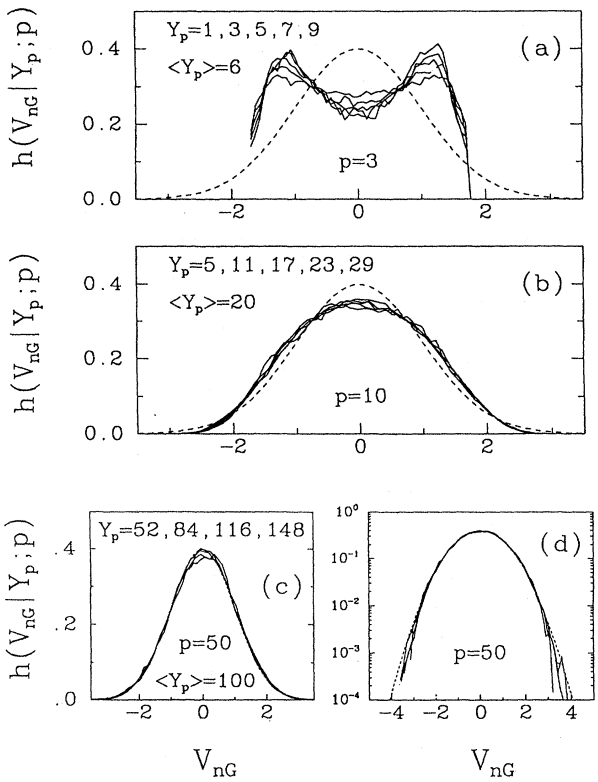

FIG. 2. Plots of $h(V_{nG}|Y_p;p)$, the conditional density of $V_{nG}=S_p/Y_p$ given Y_p, for different values of the parameter p, when the X_i are exponentially distributed. (a) $p=3$, (b) $p=10$, (c) $p=50$, and (d) $p=50$, with logarithmic ordinates. The dashed lines in each figure represent the Gaussian density with zero mean and unity variance.

the particular distribution chosen for X, although details do depend on p for small p.

A final remark is in order. The present results look similar to the central limit theorem—a special case of which states that the random variable $S_p/(p\langle X^2\rangle)^{1/2}$ has a limiting normal distribution with zero mean and unit variance for large p—but say something more because we have acquired more information by conditioning on Y_p. It is not difficult to deduce the central limit theorem from the present result that S_p/Y_p tends to a normal distribution for large p in the ensemble of S_p for *any* fixed Y_p. Now, according to the law of large numbers, the probability that $|Y_p/(p\langle X^2\rangle)-1|<\varepsilon$ (for ε as small as desired) approaches unity for sufficiently large p. Therefore the unconditional pdf of $S_p/(p\langle X^2\rangle)^{1/2}$ can be made as close as desired to the conditional pdf of S_p/Y_p at $Y_p=(p\langle X^2\rangle)^{1/2}$. Since the latter *does* tend to a Gaussian distribution with zero mean and unit variance, the central limit theorem is clearly recovered.

VI. CORRELATED PROCESSES: FRACTIONAL BROWNIAN MOTION

So far, we have considered the case of independent variables X_i (with and without the assumption of Gaussianity). In turbulence, the X_i represent velocity gradients [see the definition below Eq. (8b)] and are clearly not independent variables. The crucial question is then: What happens when correlations are allowed between X_i? In order to apply Eq. (19), we have to be able to compute $\Xi(Y_p,S_p;p)$ by performing the integral (18). That was done exactly in Sec. IV for Brownian motion, but one does not know the joint pdf $P_U(U_1,\ldots,U_p)$ for more general processes. To estimate $\Xi(Y_p,S_p;p)$ for the general case, we first note that

$$\int_{R^{p-1}} dU_2\cdots dU_p P_U\left[\frac{S_p}{\sqrt{p}},U_2,\ldots,U_p\right] = \sqrt{p}\,P_{S_p}(S_p)\,, \quad (31)$$

where the integral is taken over the $(p-1)$-dimensional hyperplane, and P_{S_p} is the pdf of S_p. Compare this with Eq. (18), which is the integral over the sphere Ω_ϕ given by the intersection of the hyperplane (8a) and the hypersphere (8b), as shown schematically in Fig. 3 for $p=3$. *We formally make the first assumption that the two integrals (18) and (31) have the same functional form.* While this appears to be reasonable, it can only be justified *a posteriori.*

We can now obtain $P_{S_p}(S_p)$ from the knowledge of the pdf of ΔZ given that $\Delta Z=KS_p$ [see Eq. (9a)]. We know from the definition of fractional Brownian motion that $\Delta Z(r)$ is Gaussian with variance $\langle\Delta Z(r)^2\rangle\sim r^{2H}$ for large r. Therefore $P_{S_p}(S_p)$ will also be a Gaussian with zero mean and variance $\langle S_p^2\rangle=K^2\langle(\Delta Z)^2\rangle \sim K^{2(H-1)}p^{2H}$. The last step uses the definition that $r=pK$.

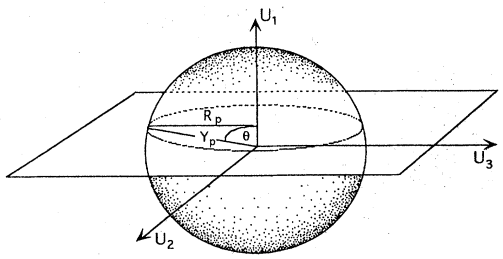

FIG. 3. The sphere represented by Eq. (8b) and the hyperplane represented by Eq. (8a) for $p=3$. The intersection of these two geometric objects constitutes the domain of integration Ω_ϕ of Eq. (18). It is characterized by Y_p and $R_p=Y_p\sin\theta$.

A suitable analytical expression for $\langle S_p^2\rangle$, valid for the entire range of p (or r),

$$\langle S_p^2\rangle\sim\frac{AK^{2(H-1)}p^2}{(B+p^2)^{1-H}}\,, \quad (32)$$

will prove useful later. As can be seen from Figs. 4(a) and 4(b), this expression fits the fractional Brownian motion data very well. In fact, a deeper reason for its choice is that a matched asymptotic analysis of structure functions in turbulence yields precisely this expression for the moments of velocity increments (Sirovich *et al.*, 1993; Stolovitzky *et al.*, 1993).

Collecting this information, we have $P_{S_p}(S_p)=\exp(-S_p^2/2\langle S_p^2\rangle)/(2\pi\langle S_p^2\rangle)^{1/2}$, with $\langle S_p^2\rangle$ given by Eq. (32). The role of p in Eq. (32) is now to set the size of the fluctuations of S_p. When the domain of integration is Ω_ϕ as in Eq. (18), the size of the fluctuations has to be

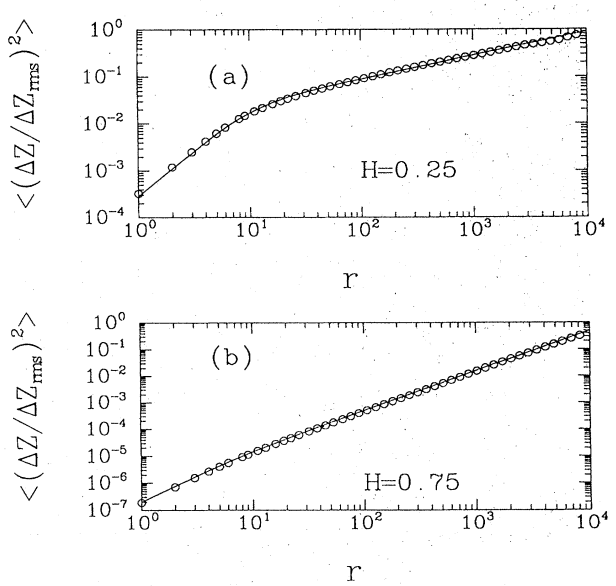

FIG. 4. The second-order moments of $\Delta Z(r)=Z(x+r)-Z(x)$, the increments of the fractional Brownian motion $Z(x)$, normalized by the root-mean-square of ΔZ (circles), and the fitting of $\langle(\Delta Z/\Delta Z_{\rm rms})^2\rangle=Ar^2/(B+r^2)^{1-H}$ (solid line). (a) $H=0.25$, $A=9.10^{-3}$, $B=100$, (b) $H=0.75$, $A=5.10^{-7}$, and $B=40$.

controlled by Y_p and R_p (see Fig. 3). Our *second assumption* is that, in identifying the integral (18) with $\sqrt{p}P_{S_p}(S_p)$, we use Eq. (32) with p replaced by Y_pR_p, even though any of the three combinations Y_p^2, R_p^2, or R_pY_p would have served in principle (since all three combinations behave approximately as $p\langle X^2\rangle$ when $p\gg 1$). Of the three combinations, we have chosen the last, which fits the data best.

The result of these two assumptions is

$$\Xi(S_p,Y_p;p)=\frac{\sqrt{p}}{\sqrt{2\pi\sigma^2(Y_p,S_p,p)}}\exp\left[-\frac{S_p^2}{2\sigma^2(Y_p,S_p,p)}\right], \tag{33}$$

where

$$\sigma^2(Y_p,S_p,p)=\frac{\sigma_0^2(Y_pR_p)^2}{[C_0+(Y_pR_p)^2]^{1-H}} \tag{34}$$

and $R_p=Y_p\sin(\theta^*)=Y_p(1-S_p^2/pY_p^2)^{1/2}$. The constants σ_0 and C_0 could be different from the constants A and B in Eq. (32), besides being p dependent in principle.

The change of variables (9), together with Eq. (19), serve to compute the pdf of $V_{\rm fBm}$ conditioned on w_r [defined just below Eqs. (9)] in the form

$$P_{\rm fBm}(V_{\rm fBm}|w_r;r)=P_1\left[\frac{V_{\rm fBm}w_r^H}{K}\middle|\frac{w_r}{15K};\frac{r}{K}\right]w_r^H/K\ . \tag{35}$$

Further, Eqs. (19), (17), and (33) yield

$$P_{\rm fBm}(V_{\rm fBm}|w_r;r)=\beta\left[1-\frac{15V_{\rm fBm}^2}{rw_r^{1-2H}}\right]^{(r/K-3)/2}\times\frac{1}{\sigma(V_{\rm fBm},w_r,r)}\times\exp\left[-\frac{V_{\rm fBm}^2}{2\sigma^2(V_{\rm fBm},w_r,r)}\right], \tag{36}$$

where β is a normalization constant,

$$\sigma^2(V_{\rm fBm},w_r,r)=\frac{\tilde{\sigma}^2(1-15V_{\rm fBm}^2/rw_r^{1-2H})}{[\tilde{C}/w_r^2+(1-15V_{\rm fBm}^2/rw_r^{1-2H})]^{1-H}}\ , \tag{37}$$

$\tilde{\sigma}=\sigma_0/15^{2H}$, and $\tilde{C}=C_0(15K)^2$. All the information about the joint pdf of the X_i needed to compute Eq. (18) has been condensed here in the three parameters $\tilde{\sigma}$, $\tilde{C}$, and K, which have to be obtained empirically.

Equations (36) and (37) show that the regimes $0<H<1/2$ and $1/2<H<1$ behave differently. In the former range of H, $P_{\rm fBm}(V_{\rm fBm}|w_r;r)$ tends to be independent of w_r and r when the latter quantities are sufficiently large, but this trend toward a unique pdf does not obtain in the latter range of H. To verify these predictions and compare Eq. (36) for $P_{\rm fBm}(V_{\rm fBm}|w_r;r)$ with the numerically generated pdfs [primarily as an *a posteriori* test of the assumptions made in evaluating the integral (18)], we produced fractional Brownian motion signals with $H=0.25$ and $H=0.75$ by the so-called *successive random addition* method (discussed, for example, by Voss 1985, 1988). For $H=0.25$ we have plotted the numerically generated pdf of $V_{\rm fBm}$ for fixed r conditioned on w_r for $r=10$ [Fig. 5(a)] and $r=50$ [Fig. 5(b)]. Each figure consists of several normalized histograms with 50 bins and was computed from at least 10^4 points. Each histogram corresponds to a particular bin of values of w_r, listed in the figure captions. For $r=10$, each w_r has a distinct pdf while for $r=50$ all pdfs collapse onto a Gaussian, except for small values of w_r. Figures 5(c) and 5(d) show the prediction of Eq. (36). The parameters $\tilde{\sigma}$, $\tilde{C}$, and K were chosen to fit the histograms for $r=10$ and were held the same for all curves with $r=50$. We observe good agreement between Eq. (36) and the numerical calculations, thus justifying the assumptions made in deriving the equation.

In contrast, the results obtained for $H=0.75$ and shown in Fig. 6(a) for $r=10$ and in Fig. 6(b) for $r=50$ yield no trend towards a unique pdf shape: from Eq. (36),

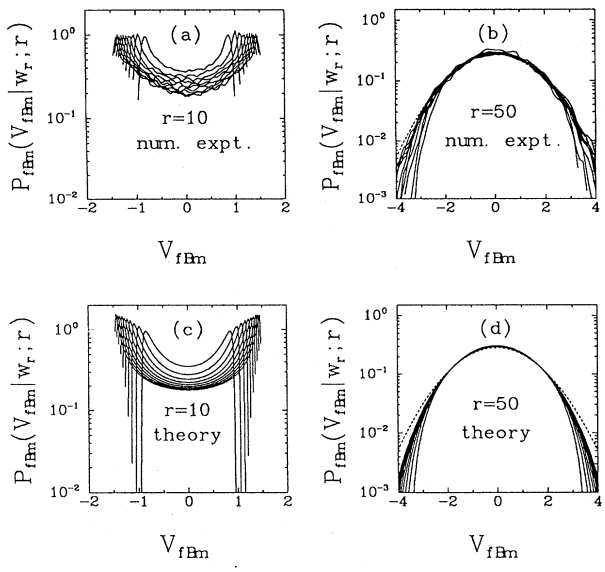

FIG. 5. Conditional probability density functions of $V_{\rm fBm}$ plotted in (a) and (b) for a numerically generated fractional Brownian motion signal with $H=0.25$. (a) $r=10$. Each curve correspondds to $w_r/\langle w_r\rangle$ held fixed in the following narrow intervals: [1,2] (innermost curve), [2,3], . . . , [10,11] (outermost curve). (b) $r=50$. Each curve corresponds to $w_r/\langle w_r\rangle$ held fixed in the narrow intervals: [10,15] (innermost curve), [15,20], . . . , [60,65] (outermost curve). (c) and (d) show corresponding theoretical predictions of Eqs. (36) and (37) for parameter values $K=15$, $\tilde{C}=7$, and $\tilde{\sigma}^2=2$: (c) $r=10$, $w_r=2,3,\ldots,11$; (d) $r=50$, $w_r=15,20,\ldots,65$. The dashed curve in (b) and (d) represents a Gaussian with a variance of 2, which is the asymptotic limit of the theoretical curve for $r\gg 1$ and $w_r/\langle w_r\rangle\gg 1$.

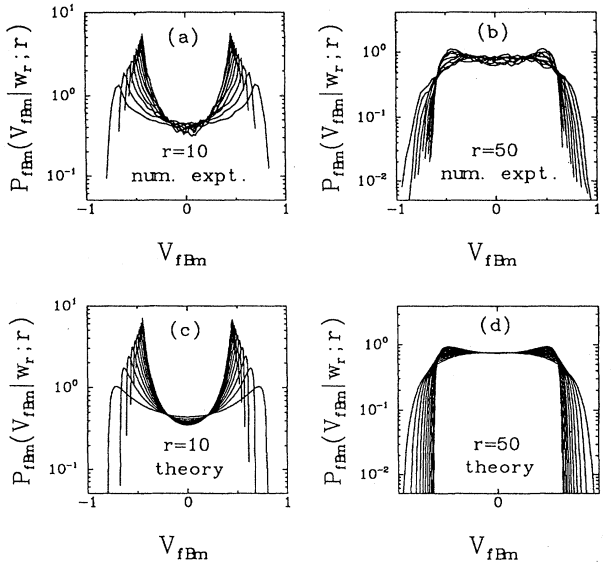

FIG. 6. Conditional probability density functions of V_{fBm} plotted in (a) and (b) for a numerically generated fractional Brownian motion signal with $H=0.75$: (a) $r=10$. Each curve corresponds to $w_r/\langle w_r\rangle$ held fixed in the following narrow intervals: [1,2] (outermost curve), [2,3], . . . , [10,11] (innermost curve). (b) $r=50$. Each curve corresponds to $w_r/\langle w_r\rangle$ held fixed in the narrow intervals: [10,15] (outermost curve), [15,20], . . . , [60,65] (innermost curve). Corresponding theoretical predictions of Eqs. (36) and (37) are plotted in (c) and (d): (c) $r=10$, $w_r=1,2,\ldots,10$ with parameter values $K=20$, $\bar{C}=0$, and $\bar{\sigma}^2=0.5$; (d) $r=50$, $w_r=10,15,\ldots,60$ with parameter values $K=50$, $\bar{C}=0$, and $\bar{\sigma}^2=0.25$.

the pdf is nonzero only over the range $V_{fBm}^2 \le r w_r^{1-2H}$, a range that shrinks with increasing w_r. Figures 6(c) and 6(d) show analytical predictions agreeing satisfactorily with the numerical data. (The set of parameters, $\bar{\sigma}$, $\bar{C}$, and K listed in the captions are different for different values of r.)

VII. HIGH-REYNOLDS-NUMBER TURBULENCE

It is helpful to restate the principal result so far, namely, that for antipersistent fractional Brownian motion the probability density function of the variable V_{fBm}, conditioned on the quantity w_r, is universal and given by Eq. (36). Since V_{fBm} is the quantity analogous to V in turbulence—and the latter plays a central role in the refined hypotheses—the principal task now is to examine the qualitative and quantitative correspondences between the conditional pdfs of V_{fBm} and of V. The basis of comparison is the following. For fractional Brownian motion, we can write $\Delta Z(r)=V_{fBm}w_r^H$, in which V_{fBm} is independent of w_r for large enough r. If this same phenomenology is assumed to hold for turbulence, we can write

$$\Delta u(r)=V(r\varepsilon_r)^H , \tag{38}$$

where V is independent of $r\varepsilon_r$ for sufficiently large r. One may ask: What is the value of H that makes the fractional Brownian motion analogy hold for turbulence, and to what range of r is the analogy applicable? From Eq. (38), the third moment of Δu can be written as

$$\langle \Delta u(r)^3\rangle = \langle V^3\rangle\langle (r\varepsilon_r)^{3H}\rangle . \tag{39}$$

Comparing this expression with Kolmogorov's (1941b) exact relation valid for inertial range turbulence (assuming, of course, that local isotropy holds),

$$\langle \Delta u(r)^3\rangle = -\tfrac{4}{5}\langle\varepsilon\rangle r , \tag{40}$$

one obtains $H=1/3$. This remark enables us to write $\Delta u(r)=V(r\varepsilon_r)^{1/3}$ in the inertial range, with V independent of $r\varepsilon_r$.

This brief discussion also points to the limitations of the comparison with turbulence. While the conditional pdf of V_{fBm} for antipersistent fractional Brownian motion is asymptotically Gaussian, it is clear from a second condition of consistency between Eqs. (39) and (40) that $\langle V^3\rangle=-4/5$, showing that the pdf of V is negatively skewed (and hence cannot be strictly Gaussian). Even so, it turns out that many features of V_{fBm} are similar to those of V. In particular, Stolovitzky *et al.* (1992) showed that the experimental V for large r is close to Gaussian in its overall shape. We shall return to the implications of this observation; at this point, it offers

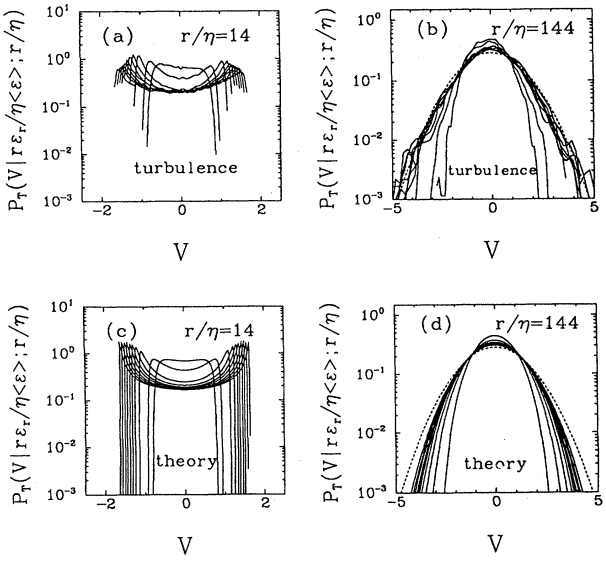

FIG. 7. Conditional probability density functions of V plotted in (a) and (b) for an atmospherical boundary layer turbulence signal: (a) $r/\eta=14$ for $r\varepsilon_r/\eta\langle\varepsilon\rangle$ in the intervals [0.1,0.5] (innermost curve), [0.5,1], [2,3], [4,5], [6,7], [8,9], [10,12], [13,15], [16,19], and [20,24] (outermost curve); (b) $r/\eta=144$ at $r\varepsilon_r/\eta\langle\varepsilon\rangle$ in the intervals [1,2] (innermost curve), [4,5], [10,11], [20,22], [30,33], [40,44], [50,55], [80,88], [120,130], and [240,270] (outermost curve). Corresponding theoretical predictions of Eqs. (41) and (42) with parameter values $K=20$, $\bar{C}=4$, and $\bar{\sigma}^2=2$ are plotted in (c) and (d). For (c) $r/\eta=14$ and $r\varepsilon_r/\eta\langle\varepsilon\rangle$ values are 0.5, 1, 3, 5, 7, 9, 12, 15, 19, and 24; (d) $r/\eta=144$ and $r\varepsilon_r/\eta\langle\varepsilon\rangle$ values are 2, 5, 11, 22, 33, 44, 55, 88, 130, and 270. The dashed curve in (b) and (d) represents a Gaussian with a variance of 2, which is the asymptotic limit of the theoretical curve for $r/\eta\gg 1$ and $r\varepsilon_r/\eta\varepsilon\gg 1$.

sufficient encouragement for exploring the application of Eq. (36) to turbulence. This exploration becomes transparent if we replace V_{fBm} by V, w_r by $r\varepsilon_r/\eta\langle\varepsilon\rangle, r$ by r/η, and H by $1/3$. Equation (36) then reads as

$$P_T[V|(r\varepsilon_r/\eta\langle\varepsilon\rangle);r/\eta]=\beta\left[1-\frac{15V^2}{\mathrm{Re}_r}\right]^{(r/K\eta-3)/2}\times\frac{1}{\sigma_T}\exp\left[-\frac{V^2}{2\sigma_T^2}\right], \quad (41)$$

where β is the normalization constant as before, $\mathrm{Re}_r=(r/\eta)(r\varepsilon_r/\eta\langle\varepsilon\rangle)^{1/3}$ is the local Reynolds number, and

$$\sigma_T^2=\frac{\tilde{\sigma}^2(1-15V^2/\mathrm{Re}_r)}{[\tilde{C}/(r\varepsilon_r/\eta\langle\varepsilon\rangle)^2+(1-15V^2/\mathrm{Re}_r)]^{2/3}}. \quad (42)$$

The detailed applicability of Eq. (41) to turbulence is what we wish to explore.

To this end, we have analyzed atmospheric turbulence data at high Reynolds numbers.[3] Defining V as in Eq. (4), we computed the experimental pdfs of V conditioned on $r\varepsilon_r/\eta\langle\varepsilon\rangle$ for different values of r. Figures 7(a) and 7(b) show these experimental results for $r/\eta=14$ and 144. The corresponding values of $r\varepsilon_r/\eta\langle\varepsilon\rangle$ are listed in the captions. Figures 7(c) and 7(d) present predictions of Eqs. (41) and (42). The parameters $\tilde{\sigma}$, $\tilde{C}$, and K were obtained by fitting with the curves for $r/\eta=14$ and then applied to $r/\eta=144$. The nearly uniform distribution for small values of $r\varepsilon_r/\eta\langle\varepsilon\rangle$ and the gradual appearance of bimodal behavior for larger values of $r\varepsilon_r/\eta\langle\varepsilon\rangle$ observed in experiment are duplicated by the formula very well. Note that the formula shows that the pdf of V is nonzero only in the interval $[-(\mathrm{Re}_r/15)^{1/2}, (\mathrm{Re}_r/15)^{1/2}]$, this being of some importance for small r. As the local Reynolds number Re_r increases, the scale for V will be given by $\tilde{\sigma}$. Such bimodality is expected at $\mathrm{Re}_r\sim 15\tilde{\sigma}^2$. When comparing Figs. 7(b) and 7(d), we observe that the trend towards the asymptotic pdf (Gaussian with $\tilde{\sigma}^2=2$ and represented by the dashed curve in both figures) emerges more slowly in the theoretical curves. This departure occurs probably because the value of K (chosen at $r/\eta=14$) is unsuitable for $r/\eta=144$. The overall features of the experimental pdfs are nevertheless well reproduced by the theory.

A further experimental aspect duplicated well by the theory is that the pdf of V for small r depends on both r and the local Reynolds number Re_r [not merely on Re_r as stated in the first hypothesis); see Stolovitzky *et al.* (1992)]. This aspect emerges clearly from Eqs. (41) and (42). For $r\gg\eta$ and $\mathrm{Re}_r\gg 1$ (more precisely, for $\mathrm{Re}_r\gg 15\tilde{\sigma}^2$), one may show $P_T(V|(r\varepsilon_r/\eta\langle\varepsilon\rangle);r/\eta)$ to tend to a Gaussian with zero mean and asymptotic variance σ_A^2 given by

$$\frac{1}{\sigma_A^2}\rightarrow\frac{15}{(r\varepsilon_r/\eta\langle\varepsilon\rangle)^{1/3}K}+\frac{(\tilde{C}/(r\varepsilon_r/\eta\langle\varepsilon\rangle)^2+1)^{2/3}}{\tilde{\sigma}^2}. \quad (43)$$

Further, σ_A^2 depends only on $r\varepsilon_r/\eta\langle\varepsilon\rangle$ and tends to $\tilde{\sigma}^2$ for big enough $r\varepsilon_r/\eta\langle\varepsilon\rangle$. This is essentially the content of the second hypothesis.

We have already pointed out that Eqs. (41) and (42) yield a symmetric V in contrast to the experiment and to the four-fifths law, both of which yield finite skewness. Operationally, the skewness information is contained in the joint pdf of $X_1,\ldots,X_p$ in Eq. (18) and can be included by using a more suitable approximation to it than Eq. (33). A Gram-Charlier expansion,[4] or some physical modeling like that used by Castaing *et al.* (1990) in the context of velocity increments would be adequate for this purpose, but the basic question remains: Why does the conditional pdf of V_{fBm} show strong similarity to turbulence even though it explicitly violates Eq. (40)—whose interpretation (Monin and Yaglom, 1971) is that it describes the energy transfer down the scales? The answer lies in the circumstance that one is examining the pdfs of V (and V_{fBm}) *conditioned* on $r\varepsilon_r$ (and w_r). *This result implies that the conditional statistics are essentially indifferent to the energy transfer process as long as one averages them properly over ensembes of fixed dissipation.*

A further difference between the fractional Brownian motion results and turbulence emerges by comparing the properties of $r\varepsilon_r$ and of its fractional Brownian motion counterpart w_r. It can be shown numerically for fractional Brownian motion (and analytically for the Brownian motion) that for sufficiently large r, $\langle w_r^q\rangle\sim r^q$ (where q is some real number), while turbulence experiments (Meneveau and Sreenivasan, 1991; Sreenivasan, 1991)

[3]Velocity measurements were made in the atmospheric surface layer at 6 m above the ground over a wheat field. The microscale Reynolds number, based on the root-mean-square velocity and the Taylor microscale, was estimated to be about 1900. Data at a microscale Reynolds number of 1500 were also acquired at about 2 m above the roof of a four-story building. Velocity fluctuations were measured using a standard hot wire (5 μm diam, 0.6 mm length) operated on a DISA 55M01 constant-temperature anemometer. The anemometer voltage was digitized on a 12-bit digitizer at sampling frequencies of 10 and 6 kHz. Some segments of the data were linearized. Further details of data acquisition and processing are given in Kailasnath (1993). For further analysis, we interpreted the time-series data as a spatial cut by invoking Taylor's frozen flow hypothesis (according to which turbulence convects undistorted at the local mean speed). Stolovitzky *et al.* (1992) provide some details of the data manipulations and a brief account of the tests made to ensure their credibility.

[4]This is a convenient and systematic way of representing a pdf that is close to the Gaussian; see, for example, Lumley (1971), Chap. 2.

show that $\langle (r\varepsilon_r)^q \rangle \sim r^{q-\mu_{3q}}$ with nonzero intermittency exponents μ_q [defined in Eq. (3)]. In the spirit of the multifractal formalism (for example, Halsey *et al.*, 1986), this implies a local scaling $w_r \sim r$ for fractional Brownian motion while $r\varepsilon_r \sim r^\alpha$ for turbulence, where the exponent α varies between $\alpha_{\min}$ and $\alpha_{\max}$, a range related to the behavior of high-order moments $\langle (r\varepsilon_r)^q \rangle$ for $q \to \pm\infty$. It is further known (Sreenivasan and Meneveau, 1988; Meneveau and Sreenivasan, 1991) that $\alpha_{\min} < 1$, emphasizing that ε_r has large excursions. For the fractional Brownian motion, on the other hand, the excursions of $w_r / \langle w_r \rangle$ are much milder.

In spite of these differences, we wish to emphasize the remarkable commonality between the fractional Brownian motion results obtained here and turbulence. Not only do the fractional Brownian motion processes possess a universal pdf for the quantity analogous to V, but their many properties are very similar for small r and for the inertial range r. Again, we are prompted to ask: How is it possible for two processes having such different statistics in one aspect ($r\varepsilon_r$ and w_r) to share (almost) the same statistics in another aspect (V and $V_{\rm fBm}$)? The key once again resides in the conditioning of the pdf. When it is conditioned on $r\varepsilon_r$ (or w_r), the features of V (or $V_{\rm fBm}$) become independent of the detailed statistics of the process. The statistics of $r\varepsilon_r$ (or w_r), however, are important when computing the unconditioned statistics of Δu (or ΔZ). It is known for turbulence (Kailasnath *et al.*, 1992) that the pdf of Δu behaves like a stretched exponential $\exp(-c|\Delta u|^\gamma)$—with stretching exponents γ depending on r and varying from $\gamma = 0.5$ for $r \sim \eta$ to $\gamma \sim 2$ for $r \sim L$—while fractional Brownian motion, by definition, possesses a Gaussian pdf of ΔZ.

Finally, we have so far concentrated on dissipative and inertial range scales without reference to scales on the order of the large scale. For such scales, $u(x+r)$ and $u(x)$ become statistically independent, and the equivalent of Eq. (32) is not valid anymore; instead, we have $\langle \Delta u(r)^2 \rangle \approx 2\langle u^2 \rangle$. One might argue on physical grounds that the same should hold for $\langle \Delta u(r)^2 | r\varepsilon_r; r \rangle$, at fixed r in the inertial range. In effect, the condition $r\varepsilon_r \gg \eta\varepsilon$ means that at least one large peak of dissipation has occurred in a segment of size r (across which the velocity increment is taken). Such peaks of high dissipation essentially separate correlated turbulent structures: The larger the dissipation in that segment, the more "different" are the structures. Such structures will have originated either from the same big structure by fragmentation and repeated processes of stretching and folding or from different large-scale structures, or both. Either situation would produce a break in correlation, as was observed in numerical experiments of Chen *et al.* (1993). This effect, as well as the inclusion of skewness, will be discussed elsewhere.

VIII. CONCLUSIONS

We have shown that an essential aspect of Kolmogorov's refined similarity hypotheses, namely, the existence of a universal variable V, holds true for more general processes than previously believed. In particular, the hypotheses apply to generic stochastic processes such as antipersistent fractional Brownian motion and classical Brownian motion. This applicability is not ubiquitous, however, because it fails to encompass persistent fractional Brownian motion. Even in the absence of precise conditions under which the refined similarity hypotheses are valid, we conjecture them to hold only for antipersistent processes. A statement with greater dynamical content must await further work.

Equations (41) and (42) appear to capture the main features of the experimental pdf $p_T(V | r\varepsilon_r/\eta\langle\varepsilon\rangle; r/\eta)$ sufficiently well, even though there are two major differences between antipersistent fractional Brownian motion and turbulence: The lack of skewness of $V_{\rm fBm}$ (while V is skewed) and the lack of multifractality of w_r/r (a known property of the box-averaged dissipation rate ε_r). The process of conditioning is thought to render these differences irrelevant to the statistical properties of V; further, the skewness can be incorporated *ad hoc* in Eq. (33), for example, by means of a Gram-Charlier expansion.

Kolmogorov's famed first and second refined similarity hypotheses appear now to stem from general stochastic principles and to be not necessarily sensitive to many aspects of Navier-Stokes equations. This is the main conceptual message we wish to convey. Actually, we think it possible to find the expression of Eq. (33) deductively by maximizing the entropy of the joint pdf of $X_1, \ldots, X_p$ conditioned on Y_p, with constraints from the second moment of S_p. The situation would then be analogous to the derivation of the Gibbs distribution in statistical mechanics (e.g., Goodstein, 1985, Chap. 1), namely, the maximization (subject to some constraints) of the entropy of the probability of the microstates, this being independent of the detailed dynamics driving the system. *If this goal can be achieved, Kolmogorov's refined similarity hypotheses will cease to be hypotheses, becoming instead theorems of the general theory of stochastic processes.*

ACKNOWLEDGMENTS

We thank Dr. D. P. Lathrop for a critical reading of a draft version and Professor M. Nelkin and Professor M. E. Fisher for some helpful remarks. The many painstaking suggestions made by Professor U. Fano significantly improved the quality of the paper. The work was supported by AFOSR and DARPA.

REFERENCES

Anselmet, F., Y. Gagne, E. J. Hopfinger, and R. A. Antonia, 1984, J. Fluid Mech. **140**, 63.

Castaing, B., Y. Gagne, and E. J. Hopfinger, 1990, Physica D **46**, 177.

Chen, S., G. D. Doolen, R. H. Kraichnan, and Z-S. She, 1993,

Phys. Fluids A **5**, 458.
Frisch, U., 1991, Proc. R. Soc. London, Ser. A **434**, 89.
Goodstein, D. L., 1985, *States of Matter* (Dover, New York).
Halsey, T. C., M. H. Jensen, L. P. Kadanoff, I. Procaccia, and B. I. Shraiman, 1986, Phys. Rev. A **33**, 1141.
Hosokawa, I., 1993, J. Phys. Soc. Jpn. **62**, 10.
Kailasnath, P., 1993, *Reynolds number effects and the momentum flux in the turbulent boundary layer,* Ph.D. thesis (Yale University).
Kailasnath, P., K. R. Sreenivasan, and G. Stolovitzky, 1992, Phys. Rev. Lett. **68**, 2776.
Kolmogorov, A. N., 1941a, Dokl. Akad. Nauk SSSR **30**, 301.
Kolmogorov, A. N., 1941b, Dokl. Akad. Nauk SSSR **32**, 16.
Kolmogorov, A. N., 1962, J. Fluid Mech. **13**, 82.
Kraichnan, R. H., 1974, J. Fluid Mech. **62**, 305.
Landau, L. D., and E. M. Lifshitz, 1963, *Fluid Mechanics* (Pergamon, London)
Lumley, J. L., 1971, *Stochastic Tools in Turbulence* (Academic, New York).
Mandelbrot, B. B., 1982, *The Fractal Geometry of Nature* (Freeman, San Francisco).
Mandelbrot, B. B., and J. W. Van Ness, 1968, SIAM Rev. **10**, 422.
Meneveau, C., and K. R. Sreenivasan, 1987, Phys. Rev. Lett. **59**, 1424.
Meneveau, C., and K. R. Sreenivasan, 1991, J. Fluid Mech. **224**, 429.
Monin, A. S., and A. M. Yaglom, 1971, *Statistical Fluid Mechanics, Vol. II* (M.I.T., Cambridge, MA).
Obukhov, A. M., 1962, J. Fluid Mech. **13**, 77.
Praskovsky, A. A., 1992, Phys. Fluids A **4**, 2589.
Sirovich, L., V. Yakhot, and L. Smith, 1993, preprint.
Sommerfeld, A., 1949, *Partial Differential Equations in Physics* (Academic, New York).
Sreenivasan, K. R., 1991, Annu. Rev. Fluid Mech. **23**, 539.
Sreenivasan, K. R., and C. Meneveau, 1988, Phys. Rev. A **38**, 6287.
Stolovitzky, G., P. Kailasnath, and K. R. Sreenivasan, 1992, Phys. Rev. Lett. **69**, 1178.
Stolovitzky, G., K. R. Sreenivasan, and A. Juneja, 1993, Phys. Rev. E **48**, R3217.
Taylor, G. I., 1935, Proc. R. Soc. London, Ser. A **151**, 421.
Thoroddsen, S. T., and C. W. Van Atta, 1992, Phys. Fluids A **4**, 2592.
Voss, R. F., 1985, in *Fundamental Algorithms in Computer Graphics,* edited by R. A. Earnshaw (Springer, Berlin), p. 805.
Voss, R. F., 1988, in *The Science of Fractal Images,* edited by H. O. Pietgen and D. Saupe (Springer, New York), p. 21.